

# Low temperature Raman spectra and energy transfer rates of ammonium nitrate polymorphic phases

Shuji Ye\*, Kenichi Tonokura\*, and Mitsuo Koshi\*

The energy transfer rates of ammonium nitrate (AN) have been studied. Line widths of Raman spectra of AN were measured as a function of temperature ranging from 3.6 to 180.0 K. The analysis of the experimental line shapes by deconvolution procedure allows to extracting a constant inhomogeneous contribution to the line broadening, due to probably crystal defects, over all the temperature range. On the basis of temperature dependence of the Raman line width of pure Lorentzian contributions, it was confirmed that the dominant mechanism for the relaxation processes of most modes were three-phonon and dephasing processes. A contribution of three-phonon down population relaxation to the line width could be separated from the contribution of dephasing processes by extrapolating the Raman line width to  $T=0.0$  K. The energy transfer rates were evaluated in terms of density of vibrational states, which were calculated using General Utility Lattice Program (GULP) codes at the pressure ranging from 0.0 to 20.0 GPa. The sum of energy transfer rates were calculated in the region  $\omega \leq 702 \text{ cm}^{-1}$  of the phases (V), (III) and (II). The results indicated that the energy transfer rates of the phases (V), (III) and (II) has a maximum value at 7.0, 11.0, and 11.0 GPa, respectively. The maximum energy transfer rates of the phases (V), (III) and (II) are 2.9, 3.6 and 11.1 times of the value at an ambient pressure, respectively.

## 1 Introduction

There has been extensive interest in the study of ammonium nitrate (AN) not only because it can be widely used as blasting agent and fertilizer, but also because it has a practical application in the field of solid oxidizers for rocket propulsion and explosive<sup>1,2)</sup>. The interest in AN as a solid oxidizer is determined by the fact that it is a cheap and safe energetic material. Moreover, unlike ammonium perchlorate, which is widely used in solid rocket propellants, AN produces less environmentally hazardous combustion products<sup>3)</sup>. In addition, as an ionic crystal, both its cations and anions are polyatomic, thus it will be an ideal prototype to study the energy transfer processes in shock-

induced detonation of energetic salts explosives.

At normal pressures, AN is known to exist in five phases in the temperature range from zero to the melting point (442.5 K). The room-temperature phase (IV) is orthorhombic with a centrosymmetric space group  $P_{mmm}(D_{2h}^{13})$  and two formula unit per unit cell<sup>4)</sup>. At temperatures below 255 K, the crystal transforms to another phase (V) and x-ray diffraction studies<sup>5) 6)</sup> show that the crystal structure undergoes a distortion into a non-centrosymmetric tetragonal structure. The reported space group of phase (V) is  $P4_2(C_4^2)$  with  $Z = 8$ <sup>5) 6)</sup>.  $Z$  is the molecular number per unit cell. On heating above room temperature, the phase transitions occur to an orthorhombic phase (III) structure at 305.3 K<sup>7)</sup>, a tetragonal phase (II) structure at 357 K<sup>8)</sup> and to a cubic phase (I) structure above 398 K<sup>9)</sup>. For the anhydrous crystals, the stability range of phase (IV) is 255-323 K<sup>3)</sup>, and with the existence of transition metal oxides such as NiO<sup>10) 11)</sup> or CuO<sup>12)</sup>, phase (IV) can

Received : May 17, 2002

Accepted : September 13, 2002

Department of Chemical System Engineering,  
University of Tokyo, 7-3-1 Hongo, Bunkyo-ku,  
Tokyo 113-8656, JAPAN

TEL:+81-3-5841-7295

FAX:+81-3-5841-7488

Email: koshi@chemsys.t.u-tokyo.ac.jp

change into phase (II) directly. It is thus clear that the phase diagram of AN is extremely complex and a complete understanding of it is difficult to be achieved<sup>3)</sup>. So the energy transfer rates under high pressure condition in its different phases will be useful to understand the shock-induced combustion and detonation of AN.

Significant process has been made in past years in the understanding of the mechanisms which regulate the dissipation of excess vibrational energy in molecular solids<sup>13)-15)</sup>. And multi-phonon up pumping mechanism<sup>16)</sup> has been proposed to explain the shock-induced detonation of explosives. However, experimental information on the energy transfer between phonon and vibron of explosives has been very limited.

Experimental information on the dynamics of a vibrational excited state can be obtained measuring directly its relaxation time by using time-resolved techniques or by line shape analysis as derived from frequency domain experiments<sup>13)-15)</sup>. These two types of experimental approaches have been widely demonstrated<sup>13)-15)</sup>. In the present study, we measured the line widths of Raman spectra of AN as a function of temperature ranging from T = 3.6 to 180.0 K. On the basis of temperature dependence of the Raman line width, it was confirmed that the dominant mechanism for the relaxation processes was three-phonon and dephasing processes. The energy transfer rates due to the three-phonon processes were evaluated in terms of density of vibrational states, which were calculated using General Utility Lattice Program (GULP) codes in phases (IV), (III), and (II) ranging from 0.0 to 20.0 GPa.

## 2 Experiment

All spectra were recorded using a double monochromator (CT-1000D, JASCO) with a CW Ar<sup>+</sup> laser (Coherent Innova70-5, 514.5 nm). The laser power was 0.25 ~ 0.45 W. The schematic of the experimental apparatus had been described in detail elsewhere<sup>17)</sup>. Monochromator slit widths were set at 50 μm, which resulted in a spectral resolution of 0.15 cm<sup>-1</sup> decided by measuring the full width at half maximum of the mode selected 514.5 nm line of the argon-ion laser. Because the

measured spectra interval is 0.05 cm<sup>-1</sup> and the experimental resolution is well below the observed line widths, so that no deconvolution of the measured line shapes with instrumental function was necessary. Samples were cooled down to 3.3 K using a cryogenic refrigerator (PS24SS, Nagase & Co. Ltd.) for optical measurements. The samples (Aldrich, 99.99+%) were used with three-time re-crystallization in a saturated aqueous solution.

For an actual crystal, there is another source of line broadening is due to the presence of the inhomogeneities. The homogeneous line shape function is Lorentzian whereas the inhomogeneous line shape function is Gaussian. In the case of a homogeneous line broadening and pure Lorentzian shape the full width  $\gamma$  is related to the lifetime  $\tau$  by the expression  $\gamma=1/(\pi c \tau)$ , where  $c$  is the speed of light. As pointed out by Califano et al.<sup>19)-22)</sup>, the deconvolution of the experimental line shapes allows to extracting a constant inhomogeneous contribution to the line broadening using a Voigt line-shape function.

$$I^{obs}(\omega) = \int I^{hom}(\omega - \omega_0) I^{inhom}(\omega_0) d\omega_0 = \int I^L(\omega - \omega_0) I^G(\omega_0) d\omega_0 \quad (1)$$

where  $I^{obs}(\omega)$ ,  $I^{hom}(\omega)$ ,  $I^{inhom}(\omega)$ ,  $I^L(\omega)$  and  $I^G(\omega)$  are the observed, homogeneities, inhomogeneities, Lorentzian and Gaussian line shape, respectively. The line widths of Lorentzian and Gaussian components were obtained from the fittings. An typical example is shown in Fig. 1.

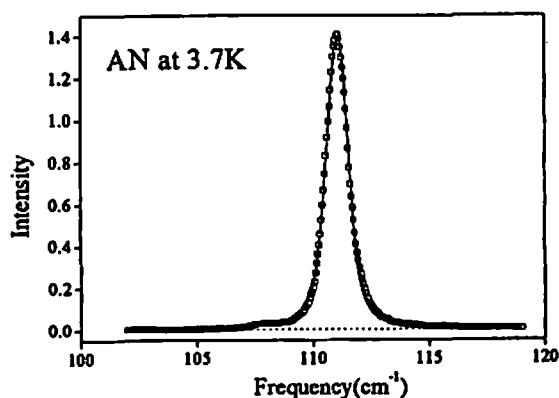


Fig.1 The example of Voigt fitting.

## 3 Calculation method

The calculations of density of vibrational states performed were done using the software package of GULP codes<sup>23) 24)</sup>. In the present calculations,

Table.1 The intermolecular potential parameters of AN<sup>a)</sup>

bond	Phase (V)		Phase (III)		Phase (II)	
	A	B	A	B	A	B
N-N	1904534. 6	1508. 9	1904534. 6	1508. 9	1904534. 6	1508. 9
O-O	1970959. 87	2739. 5	1970959. 87	2739. 5	1970959. 87	2739. 5
H-H	2195. 37	124. 87	2195. 37	124. 87	2195. 37	124. 87
N-O	3735452. 02	3484. 43	5473987. 07	2685. 5	4074958. 68	2299. 56
N-H	100441. 03	454. 45	100441. 03	2673. 61	100441. 03	454. 45
O···H*	1662. 97	674. 54	75853. 5	10984. 91	1662. 97	674. 54

<sup>a)</sup> A and B denote the Lennard-Jones potential parameters as described in ref.3, unit is in kJÅ<sup>12</sup> for A and kJÅ<sup>6</sup> for B. The corresponding hydrogen potential parameters are indicated by an asterisk, unit is in kJÅ<sup>10</sup> for A and kJÅ<sup>6</sup> for B.

we locate molecules based on covalent radii and retain all Coulomb interaction within the molecule, and then exclude the intramolecular Coulomb potential. The cut-off distance  $R_{cut} = 40.0\text{Å}$  was used to provide accurate summation of the intermolecular potential.

The potential functions used to describe the intermolecular interactions in crystalline AN were constructed as a sum of pairwise additive Lennard-Jones(LJ), hydrogen bonding (HB) and Coulombic (C) potentials of the form. The intramolecular interaction potential includes the stretching, bending and torsional motion (only for the case of NO<sub>3</sub>) of the isolated ions. The parameters of the intermolecular and intramolecular potentials had been published by Thompson et al.<sup>3)</sup> to calculate the lattice energy of phase (V). In the present calculations, we used the potential parameters without any change for phase (V) and refitted the pair of atoms N···O, N···H and O···H intermolecular potentials for phase (III) and phase (II). The intermolecular potential parameters after fitting were given in Table 1. Intramolecular potential parameters were the same with reference 3.

## 4 Results and discussion

### 4.1 Raman line widths

There have been many studies<sup>25)-27)</sup> for low temperature Raman and infrared spectra of AN. We measured the line widths for several phonon and vibron modes as a function of temperature ranging from T = 3.6 to 180.0 K. The results indicated that some of them show square

dependence on temperature while the others have a linear dependence in the classical regime ( $\hbar\omega < \kappa_B T$ ). Based on a relaxation theory<sup>13)-15)</sup>, the line width is written as the sum of contributions from phonon down and up relaxation processes and pure dephasing processes at low temperatures.

$$\gamma = \gamma_{3d} + \gamma_{3u} + \gamma_{deph} + \gamma_{4d} \quad (2)$$

$$\gamma_{3d} = B_{3d}(n_i + n_j + 1) \quad (3)$$

$$\gamma_{3u} = B_{3u}(n_i - n_j) \quad (4)$$

$$\gamma_{4d} = B_{4d} \{ (n_i + 1)(n_j + 1)(n_k + 1) - n_i n_j n_k \} \quad (5)$$

$$\gamma_{deph} = B_{deph} n_i (n_i + 1) \quad (6)$$

$$n_i = 1 / [\exp(\hbar\omega_i / \kappa_B T) - 1] \quad (7)$$

where the  $B_{3d}$ ,  $B_{3u}$ ,  $B_{4d}$  and  $B_{deph}$  are the usual third-order, fourth-order and dephasing anharmonic terms of the crystal Hamiltonian, respectively, and  $n_i$  is the occupation number of phonon,  $\omega_i$  is a frequency of  $i$ -th phonon mode.

Since the occupation number is proportional to T when  $\hbar\omega < \kappa_B T$ , the values of  $\gamma_{3d}$  and  $\gamma_{3u}$  depend linearly on temperature, whereas the values of  $\gamma_{deph}$  and  $\gamma_{4d}$  depend on T<sup>2</sup>. Because of this difference in temperature dependence, it is possible to separate the contribution of three-phonon relaxation to the line width from the contribution of dephasing process by extrapolating the Raman line width to T=0.0 K. Those observed non-linear dependences in the temperature range of  $\hbar\omega < \kappa_B T$  indicate the occurrence of fourth-order processes.

As has been discussed in previous studies<sup>28)-32)</sup>, the identification of the actual relaxation pathways is a complicated task since it may involve the contribution of several processes and terms of the anharmonic Hamiltonian. However, a qualitative

Table.2 Anharmonic coefficients and phonon frequencies at 0.0 K for phonon and vibron relaxation processes in AN (V) crystal<sup>a)</sup>.

$\nu$	$B_{3d}$	$\omega_1$	$B_{\text{deph}}$	$\omega$	$B_{3u}$	$\omega_1$	$B_{4d}$	$\omega_1$	$\omega_2$
48.7	0.15	24.5	0.032	12	-	-	-	-	-
74.3	0.175	24.5	0.11	24.5	0.175	24.5	-	-	-
86.7	0.25	43.5	0.6	49.0	0.5	24.5	-	-	-
97.8	0.24	49.0	-	-	-	-	0.11	24.5	24.5
111.0	0.60	49.0	-	-	2.25	49	-	-	-
139.7	2.4	111.0	-	-	-	-	-	-	-
710.3	-	-	0.05	49.0	-	-	0.63	231.0	231.0
1294.0	2.1	231.0	-	-	1.5	49.0	-	-	-
1406.4	2.1	95.0	-	-	0.7	24.5	-	-	-
1414.7	2.0	7.5	0.16	24.5	-	-	-	-	-
1446.0	1.05	61	-	-	-	-	-	-	-

<sup>a)</sup> unit is in  $\text{cm}^{-1}$ , in  $B_{3d}$  process,  $\omega_2 = \nu - \omega_1$ ; in  $B_{3u}$  process,  $\omega_2 = \nu + \omega_1$ ; in  $B_{4d}$  process,  $\omega_3 = -\nu - \omega_1 - \omega_2$

picture of the relaxation mechanisms can be obtained in term of the simplest process considering the anharmonic coupling coefficients as fitting parameters<sup>18),22)</sup>. In the depopulation mechanisms, up-conversion processes predict  $\gamma_{3u}$  and  $\gamma_{\text{deph}} = 0$  at 0 K; consequently only down-conversion processes contribute to the line broadening for temperature close to 0 K. As pointed out by Califano and Schettio<sup>11)</sup>, three-phonon depopulation processes are more probable than higher order decay processes. Therefore we used three-phonon down processes to fit the residual line width at low temperature for most modes. The increase in the temperature causes the thermal bath to be progressively populated, determining the activity of the up-conversion processes, which must also be included in the fit of the line width. Quartic conversion processes are inserted only for these modes having non-linear temperature dependences of the line width. The simplest fourth-order process is the dephasing process, which is expected to be the most efficient for a vibron relaxation<sup>33)</sup>. Based on the measured energy levels of the phonons and vibrons, the line width of some phonons and vibrons has been interpreted using eqs.(2)-(7). For example, the vibron mode at  $1406.0 \text{ cm}^{-1}$  down converts to vibron at  $1311 \text{ cm}^{-1}$  and creates a phonon at  $95 \text{ cm}^{-1}$ . As temperature increases, it up-converts to a vibron at  $1431 \text{ cm}^{-1}$  and absorbs a phonon of  $24.5 \text{ cm}^{-1}$ . The results of relaxation processes are given

in Table2. For the lowest frequency vibron at  $710.0 \text{ cm}^{-1}$ , because the maximum frequency of phonon is about  $246 \text{ cm}^{-1}$ , it can only relax itself by four-phonon processes and dephasing processes. The results in Table 2 indicated that the dominant mechanisms for the relaxation processes of most modes were three-phonon and dephasing processes.

#### 4.2 Energy transfer rates

As discussed in section 4.1, on the basis of the temperature dependence of the line width, three-phonon and dephasing processes would be the dominant relaxation mechanism for the most of phonons and vibrons of AN. Since the dephasing can occur by a pure transverse relaxation in which no energy exchange (dissipation) occurs but only dynamic fluctuations destroy the phase relationship<sup>34)</sup>, then we can consider the main contributions to energy transfer rates are due to three-phonon processes. Although three-phonon processes include energy-down transfer and energy-up transfer processes, since the energy must be transferred to the bond stretching modes relevant to bond breaking<sup>35)</sup>, hence we will fix the energy of a given phonon or vibron state  $\omega_3$  and sum over all phonons or vibrons ( $\omega_1, \omega_2$ ) such that  $\omega_1 + \omega_2 = \omega_3$ . It is said, we only consider the energy transfer from low-frequency modes ( $\omega_1, \omega_2$ ) to high-frequency modes ( $\omega_3$ ).

Fried and Ruggiero<sup>35)</sup> have derived a simple

formula for the phonon up-conversion rates into a given vibron mode. According to their formula, for a given band  $\omega_c$ , the energy transfer rates per a volume of crystal is given as follows,

$$\kappa(\omega_c, T) = \frac{9|B|^2}{4\pi^2 \rho_0 \hbar^2} \int d\omega \tilde{n}(\omega) \tilde{n}(\omega_c - \omega) \rho(\omega) \rho(\omega_c - \omega) \quad (8)$$

where,  $\rho_0$  is the density of sample, B is cubic anharmonic coupling coefficient,  $\rho(\omega)$  is the phonon or vibron density of states, defined by

$$\rho(\omega) = \sum_j \int dk \frac{\delta(\omega - \omega_j(k))}{8\pi^3} \quad (9)$$

In order to compare the energy transfer rates from different molecules or different phases for the same molecule, it is necessary to determine a normalization factor. The simplest alternative is to take the integral of  $\rho(\omega)$  over all frequencies to be equal to  $3N/V_c$ , where N is the number of atoms per unit cell and  $V_c$  is the volume of unit cell.

At ambient pressure, according to the assumption of Fried and Ruggiero<sup>35)</sup>, we also assume that the anharmonic coupling per molecular volume is the same for different phases, this is equivalent to taking  $B = V_c B_0 / Z$ , where Z is the number of molecules per unit cell. Then eq.(8) can be written as:

$$\kappa(\omega_c, T) = \frac{81 B_0^2 N^2}{4\pi^2 \rho_0 \hbar^2 Z^2} \int d\omega \tilde{n}(\omega) \tilde{n}(\omega_c - \omega) \rho(\omega) \rho(\omega_c - \omega) \quad (10)$$

where,  $\int d\omega \rho(\omega) = 1$  over all frequencies.

In the region of  $\kappa_B T \gg \hbar \omega$ ,  $\tilde{n}(\omega) \approx [\exp(\hbar\omega/(\kappa_B T)) + 1]^{-1} \approx \kappa_B T / (\hbar\omega)$ , then eq.(10) changes into eq.(11).

$$\kappa(\omega_c, T) = \frac{81 B_0^2 \kappa_B^2 T^2 N^2}{4\pi^2 \rho_0 \hbar^4 Z^2} \int d\omega \frac{\rho(\omega) \rho(\omega_c - \omega)}{\omega(\omega_c - \omega)} \quad (11)$$

At high pressures, B increases with the compression due to the decrease in intermolecular separation<sup>36)</sup>. We derived the eq.(12) for the energy transfer rates at high pressures according to reference 16.

$$\kappa(V, \omega_c, T) = \frac{81 B_0^2 \kappa_B^2 T^2 N^2}{4\pi^2 \rho_0 \hbar^4 Z^2} \left(\frac{V_0}{V}\right)^6 \int d\omega \frac{\rho(\omega) \rho(\omega_c - \omega)}{\omega(\omega_c - \omega)} \quad (12)$$

where  $V_0$  is the volume of unit cell at  $P = 0$  GPa, and V is the volume of unit cell at the pressure P.

Using eqs. (11) and (12), the energy transfer rates

are calculated in terms of the phonon and vibron density of states(DOS). The results are given in Fig.2. We calculated the sum of energy transfer rates in the region  $\omega \leq 702 \text{ cm}^{-1}$  and found that it accounts for more than 70% of the whole energy transfer rates over all frequencies. It is noted that the region  $\omega \leq 702 \text{ cm}^{-1}$  corresponds to "doorway" region defined by Dlott et al.<sup>16) 36)</sup>. The "doorway" region plays an important role in shock-induced detonation.

In the shock-induced experiments, a sudden high pressure is generated. Compressing the materials increases the number of phonons per unit volume, but induces the frequency shifts to higher energy level. In general, the shifts of phonon modes are much greater than that of vibrational modes. Then the modes lying in the region  $\omega \leq 702 \text{ cm}^{-1}$  are

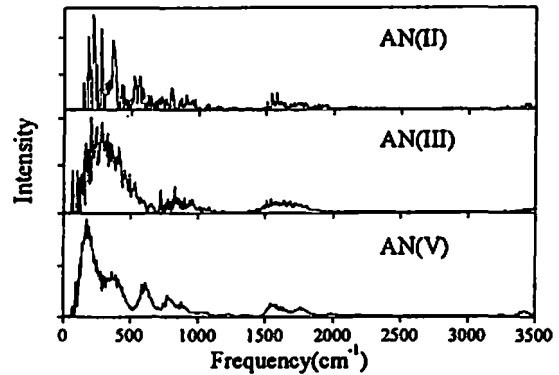


Fig.2 The calculated energy transfer rates of AN at ambient pressure and room temperature.

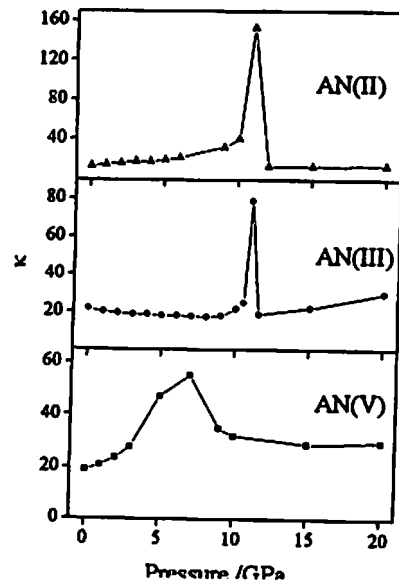


Fig.3 The calculated energy transfer rates of AN as a function of pressure at room temperature.

decreased. In addition, due to the frequencies move to higher energy level, the number of phonons or vibrons per unit frequency interval decreases. Then the excitation possibility will have a maximum value at some pressure. The excitation possibility is defined as  $\int d\omega \rho(\omega) \rho(\omega_c - \omega) / [\omega (\omega_c - \omega)]$ , where  $\int d\omega \rho(\omega) = 1$  over all frequencies. To understand the energy transfer rates under the high pressure condition, we calculate the phonon and vibron DOS and energy transfer rates as a function of pressure. The sum of energy transfer rates in the region  $\omega \leq 702 \text{ cm}^{-1}$  are shown in Fig.3. It is very interesting for that the energy transfer rates of AN(V), AN(III), and AN(II) have a maximum value at 7.0, 11.0 and 11.0 GPa respectively. The maximum energy transfer rates of AN(V), AN(III) and AN(II) are 2.9, 3.6 and 11.1 times of the value at ambient pressure conditions. The results indicate that the phase AN(II) is more easy to explode under high pressures than other two phases. However, no experimental data at a high pressure was available for comparison.

#### Conclusions

The line widths of Raman spectra of AN were measured over the temperature range 0–180 K. On the basis of line-shape analysis, it was confirmed that the dominant mechanism for the relaxation processes of most modes were three-phonon and dephasing processes. The energy transfer rates of the phases (V), (III) and (II) has a maximum value at 7.0, 11.0, and 11.0 GPa, respectively. The maximum energy transfer rates of the phases (V), (III) and (II) are 2.9, 3.6 and 11.1 times of the value at an ambient pressure, respectively. It is indicated that the phase AN(II) is more easy to explode under high pressures than other two phases.

#### References

- 1) C. Oommen, S.R. Jain, *J. Hazardous Mater.* 67: 253(1999).
- 2) B.N. Kondirkov, V.E. Annikov, V.Y. Egorshv, L. Deluca, C. Bronzi, *J. Propulsion Power* 15:763(1999).
- 3) D.C. Sorescu, D.L. Thompson, *J. Phys. Chem. A* 105: 720(2001).

- 4) C.S. Choi, J.E. Mapes, E. Prince, *Acta Crystallogr.* B28:1357(1972).
- 5) J.L. Amorós, F. Arrese, M. Canut, *Z. Kristallogr.* 117: 92(1962).
- 6) C.S. Choi, H.J. Prask, *Acta Cryst.* B39: 414 (1983).
- 7) B.W. Lucas, M. Ahtee, A.W. Hewat, *Acta Cryst.* B36: 2005(1980).
- 8) B.W. Lucas, M. Ahtee, A.W. Hewat, *Acta Cryst.* B35: 1038(1979).
- 9) Y. Shinnaka, *J. Phys. Soc. Jpn.* 4: 073 (1959).
- 10) C.S. Choi, H.J. Prask, E. rince, *J. Appl. Crystallogr.* 13: 403(1980).
- 11) W. Engle, *Explosivstoffe* 1: 9(1973).
- 12) F.J. Owens, *J. Appl. Phys.* 53: 368 (1982).
- 13) A. Laubereau, W. Kaiser, *Rev. Mod. Phys.* 50, 607(1978).
- 14) S. Califano, V. Schettino, *Int. Rev. Phys. Chem.* 7:19(1988).
- 15) S. Califano, V. Schettino, N. Neto, *Lattice dynamics of molecular crystals*, vol.26 in Springer series on Lecture notes in Chemistry, edited by G. Berthier, et al. (Springer, Berlin, 1981).
- 16) D.D. Dlott, M.D. Fayer, *J. Chem. Phys.* 92: 3798(1990).
- 17) S. J. Ye, K. Tonokura, M. Koshi, *J. Jpn. Explos. Soc.* 63:49(2002).
- 18) R. Bini, *J. Chem. Phys.* 104: 4365(1996).
- 19) C. Panero, R. Bini, V. Schettino, *J. Chem. Phys.* 100:7938(1994).
- 20) L. Poletti, R. Bini, V. Schettino, *Chem. Phys. Lett.* 222:239(1994).
- 21) L.A. Hess, P.N. Prasad, *J. Chem. Phys.* 72:573 (1980).
- 22) J.C. Bellows, P.N. Prasad, *J. Chem. Phys.* 70:1864(1979).
- 23) J.D. Gale, *J. Chem. Soc., Faraday Trans.* 93: 629(1997).
- 24) J.D. Gale, *Philos. Mag.* B73:3(1996).
- 25) Y.S. Park, J.K. Reid, R.J.C. Brown, H. F. Shurvell, L.J. Norrby, *J. Raman Spectr.* 23: 697(1992).
- 26) Z.X. Shen, M.H. Kuok, S.H. Tang, W. F. Sherman, *Spectrochimica Acta* 49A:21(1993).
- 27) H.C. Tang, B.H. Torrie, *J. Phys. Chem. Solids* 39: 845(1978).

- 28) R. Bini, Chem.Phys. 84: 97(1980).  
29) P.Foggi, V. Schettino, Nuo Cimento, 15:7(1992).  
30) V.K.Jindal, R.Righini, S.Califano, Phys. Rev. B 38: 4259(1988).  
31) P.Procacci, G.Cardini, R.Righini, S.Califano, Phys. Rev.B 45:2113(1992).  
32) P.Procacci, G.F.Signorini, R.G. Della Valle, Phys.Rev. B 47:11124(1993).  
33) J.P. Pinan, R. Ouillon, P. Ranson, M. Becucci and S.Califano, J.Chem.Phys. 109:5469 (1998).  
34) J.C.Bellows, P.N.Prasad, J. Chem. Phys. 70 : 1864(1979).  
35) L.E.Fried, A.J.Ruggiero, J. Phys. Chem. 98 : 9786(1994).  
36) A.Tokmakoff, M.D.Fayer, D.D.Dlott, J.Phys. Chem. 97: 1901(1993).
-